Transformation quantum optics: designing spontaneous emission using coordinate transformations

2016 J. Opt. 18 044029

(http://iopscience.iop.org/2040-8986/18/4/044029)

IOP Publishing Journal of Optics
J. Opt. 18 (2016) 044029 (11pp) doi:10.1088/2040-8978/18/4/044029

Transformation quantum optics: designing spontaneous emission using coordinate transformations

Jingjing Zhang[1,2], Martijn Wubs[2], Pavel Ginzburg[1,3], Gregory Wurtz[1] and Anatoly V Zayats[1]

[1] Department of Physics, King's College London, Strand, London WC2R 2LS, UK
[2] Technical University of Denmark, Department of Photonics Engineering-DTU Fotonik, Lyngby, 2800, Denmark
[3] School of Electrical Engineering, Tel Aviv University, Tel Aviv 69978, Israel

E-mail: jinz@fotonik.dtu.dk

Received 15 October 2015, revised 16 November 2015
Accepted for publication 20 November 2015
Published 1 April 2016

Abstract

Spontaneous decay is a fundamental quantum property of emitters that can be controlled in a material environment via modification of the local density of optical states (LDOS). Here we use transformation optics methods in order to design required density of states and thus spontaneous emission (SE) rate. Specifically, we show that the SE rate can be either enhanced or suppressed using invisibility cloaks or gradient index lenses. Furthermore, the anisotropic material profile of the cloak enables the directional control of SE. We also discuss how the practical issues, such as dispersion and losses, affect the LDOS in complex materials. Tailoring SE properties using transformation optics approach provides an innovative way for designing emission properties in a complex material environment needed for the development of active nanophotonic devices.

Keywords: transformation optics, spontaneous emission, density of optical states, invisibility cloaks

(Some figures may appear in colour only in the online journal)

Introduction

In both quantum and conventional photonic technologies, the ability to control light emission is a cornerstone of many modern applications. Lasers and optical amplifiers, optical and plasmonic nanolasers and spasers, single and entangled photon sources required for telecommunications and quantum information processing rely on this ability. The properties of spontaneous emission (SE), which is a purely quantum mechanical process and which influences also stimulated emission, can be modified by engineering the photonic density of states at the emission wavelength [1]. Traditionally, the photonic density of states can be modified from its free space (uniform dielectric medium) value in structured environment using, e.g., micro- and nano-cavities [2], optical antennas [3] or generally near the material boundaries [4, 5]. Both dielectric [6] and plasmonic micro- and nanostructures, such as photonic crystals [7–9], plasmonic waveguides [10], plasmonic nanoantennas [11, 12], microcavities [13], and metamaterials [14], have been employed for this purpose. In a weak coupling regime between an emitter and nanostructure [15], the lifetime and, thus, radiation rate of the emitter, is then determined by the so-called Purcell factor [16] related to the increased or decreased density of states at the position of the emitter in the structured environment. The simplest well-known example is the increased rate of the SE in the sub-wavelength proximity to metal surfaces where the density of states is increased due to surface plasmon polariton modes [4]. Giant Purcell factors have been recently predicted in the so-called hyperbolic metamaterials of different realizations [14, 17–19]. Such metamaterials are also suitable for designing invisibility cloaks [20, 21].

In many cases the photonic environment is used to achieve the increased density of states and the increased SE rate [2, 13, 14]; sometimes this happens by the nature of the nanostructures and may not be desirable, e.g., in nanolasers or

spasers where the increased rate of SE may compete with the stimulated emission, while in other cases it helps to depopulate long-lived excited states which are responsible for degradation of polymer materials [22] or increase of two-photon emission efficiency [23]. In many applications, the suppressed SE may be advantageous where long-lived excited states are required. This is needed for improving lasing or spasing conditions, design of deterministic single photon sources for quantum information processing and optical memory for telecom applications, to name a few.

The recent developments in transformation optics have provided a powerful tool for designing controlled flow of electromagnetic waves with a varying refractive index profile [24–33] and designing surface plasmon resonances of complex nanostructures [34–40]. Electromagnetic devices such as invisibility cloaks [24–28], lenses [29–31], field rotators [27], antennas [32, 33], and many others have been engineered. Such designs generally require materials with specific optical properties, but these can, in turn, be achieved using metamaterial approaches [41]. Significant progress has also been made in using transformation optics for rigorous studies of plasmonic nanostructures which are difficult to consider with traditional theoretical approaches [35–40]. While numerous applications have been discussed in the realm of classical optics, limited attention has been paid to the capabilities of transformation optics with respect to quantum optical processes.

In this paper, we study how to design the local density of optical states (LDOS) which determines SE properties, using a transformation optics approach, and discuss the impact of practical issues, such as dispersion and damping, on LDOS. Specifically, we investigate the control of SE with different devices designed with transformation optics. We show that the SE rate can be either enhanced or suppressed using invisibility cloaks [24–28] or gradient-index lenses [29–31]. Furthermore, the anisotropic material profile of the cloak can enable the directional control of the SE rate. The described effects open up new possibilities to implement nanophotonic components both for passive and active control of SE inside metamaterials, which have started to make their way in practical photonic devices.

Transformation optics approach

The rate of SE can be modified by placing the emitter in a specially structured environment. In the simplest case, the radiation enhancement factor (the Purcell factor) is a property of a cavity and, in the case of a weak coupling regime, can be defined as the ratio of the SE rate inside the cavity Γ to that in the free space Γ_0 [42]: $F_p = \frac{\Gamma}{\Gamma_0} = \frac{3Q}{4\pi^2 V}\left(\frac{\lambda}{n}\right)^3$, where Q and V are the quality factor and mode volume of the cavity, respectively, λ is the wavelength of the emitted light in vacuum, and n is the refractive index of material. Fermi's golden rule dictates that the transition rate for the atom-vacuum (or atom-cavity) system is proportional to the density of final states. In a cavity at resonance, the density of final states is increased (though the number of final states may not be). The Purcell factor is then related to the ratio of the cavity and free space density of states.

In a homogeneous medium, LDOS describes the number of allowed states at a certain frequency within the volume $[k_\omega, k_{\omega+\Delta\omega}]$ in the wavevector k space:

$$\rho = \frac{1}{\pi^3}\frac{\mathrm{d}\Omega_{k(\omega)}}{\mathrm{d}\omega}, \tag{1}$$

where ρ is the LDOS, ω is the angular frequency of the electromagnetic wave, and $\Omega_{k(\omega)}$ represents the reciprocal volume contained within the isofrequency contour k_ω.

The LDOS can be modified by changing the environment where the emitter is placed. Let us consider a transformation which maps the space (x, y, z) to the space (x', y', z'): $\mathrm{d}\bar{r}' = \bar{\bar{A}} \cdot \mathrm{d}\bar{r}$, where $A = \partial(x', y', z')/\partial(x, y, z)$ is the Jacobian matrix of the transformation function. Because the transformation does not introduce extra reflections, the total number of states is preserved, whereas the space is compressed (or expanded). Thus, the LDOS in the transformed coordinate is given by (see appendix for derivations)

$$\rho' = \det{}^{-1}\left(\bar{\bar{A}}\right)\rho. \tag{2}$$

As seen from equation (2), the LDOS associated with the transformed medium is proportional to $\det^{-1}(\bar{\bar{A}})$, indicating that the LDOS can be engineered directly by a distortion of space. Figure 1 illustrates modification of the LDOS in the medium under coordinate transformation. Assuming the medium in the initial space to be isotropic, the LDOS corresponds to the number of states that are contained in the brown annulus region of the left panel in figure 1. After the transformation, the iso-frequency contour in k-space changes as shown in the right panel. If the space is compressed, the LDOS is enhanced by the compression factor. On the other hand, the LDOS is decreased if the space is expanded.

In the general case of an arbitrary inhomogeneous medium, the LDOS can be deduced from the imaginary part of the Green's function [1, 43]:

$$\rho = \frac{2k}{\pi v_g}\lim_{\bar{r}\to\bar{r}_0}\mathrm{Im}\left[\mathrm{Tr}\,\overleftrightarrow{G}(\bar{r}, \bar{r}_0)\right], \tag{3}$$

where $\overleftrightarrow{G}(\bar{r}, \bar{r}_0)$ stands for the Green's function and v_g is the group velocity. The Green's function associated with the transformed space is deduced as (see appendix for derivations)

$$\overleftrightarrow{G}'(\bar{r}', \bar{r}'_0) = \left(\overline{\overline{A}}^T\right)^{-1} \cdot \overleftrightarrow{G}(\bar{r}, \bar{r}_0) \cdot \overline{\overline{A}}^{-1}. \tag{4}$$

Thus, the decay rate of the emitter as well as related broadening and shift of the resonance which all are related to the Green's function can be designed by prescribed coordinate transformation, in the same way as refractive index variations are designed. The modification of the SE rate under the space transformation in the lossless case can then be expressed as

$$\Gamma' = \frac{|A^{-1} \cdot p|^2}{|p|^2}\Gamma, \tag{5}$$

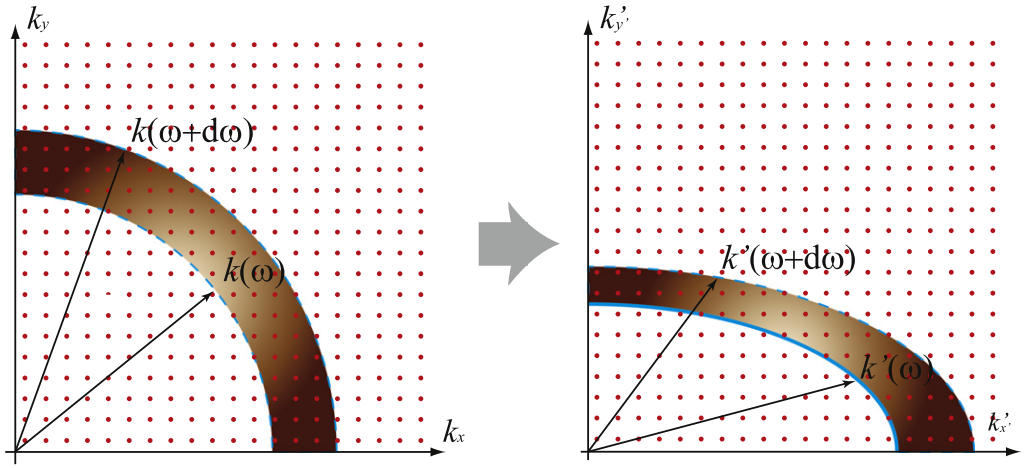

Figure1. LDOS (denoted by shaded area) in the original space and after the transformation.

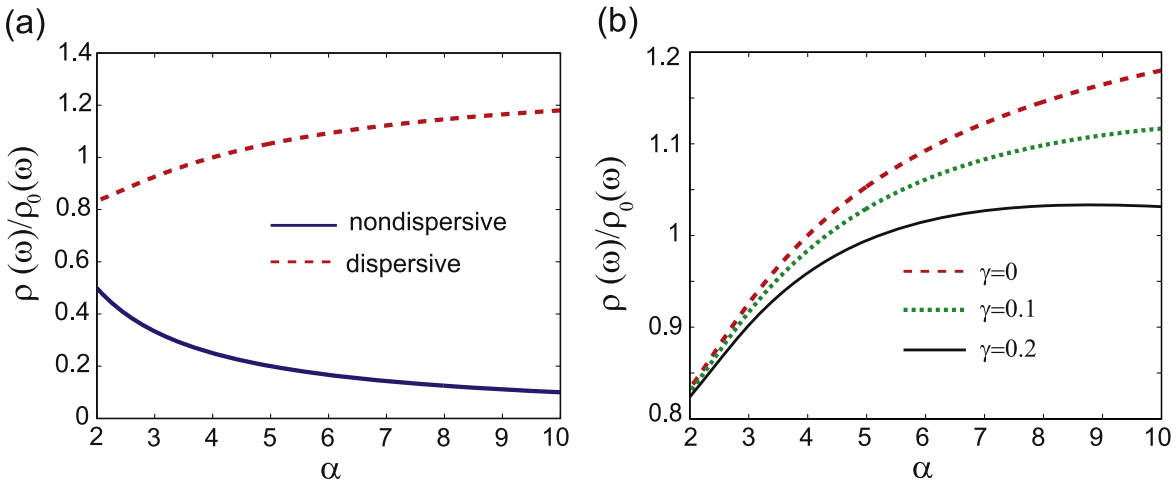

Figure 2. LDOS dependence on the expansion factor α in the linear transformed space. (a) The comparison of LDOS in nondispersive and dispersive cases without dissipation. (b) The comparison of LDOS in dispersive media with different damping frequencies.

where p is the dipole moment of the emitter (see appendix for derivations).

To provide an intuitive understanding of equations (2) and (5), we consider a simple distortion of free space $x' = \alpha x$, $y' = \alpha y$, $z' = \alpha z$, where α is the compression/expansion factor of the space. According to the transformation optics theory, the material in the new space has a homogeneous isotropic permittivity and permeability with $\varepsilon' = \mu' = \frac{1}{\alpha}$. The LDOS is $\rho' = \alpha^{-3}\rho$ and the SE is modified as $\Gamma' = \alpha^{-2}\Gamma$ in the transformed space given by equation (5). (This result also agrees with the previous studies in [44, 45]). This indicates that we can enhance/suppress the SE rate by properly compressing/expanding the surrounding space. In a more complicated case, a coordinate transformation may lead to an anisotropy if only one axis is compressed/expanded: $x' = \alpha x$, $y' = y$, $z' = z$, leading to the anisotropic material profile in the new space: $\varepsilon'_x = \mu'_x = \alpha$, $\varepsilon'_y = \mu'_y = \varepsilon'_z = \mu'_z = \alpha^{-1}$. The LDOS is then modified as $\rho' = \alpha^{-1}\rho$ in the transformed space (equation (2)). If $\alpha > 1$, corresponding to an expansion of space, the LDOS will be suppressed by the factor of α and thus will be smaller than that in free space, as depicted by the blue solid curve in figure 2(a). Note that the increase of α results in the decrease of transformed refractive index, and, therefore, the LDOS in transformed space.

The anisotropic material profile in the transformed space can be realized with metamaterials which are usually dispersive and lossy. Therefore, we need to account for the impact of dispersion and damping on the change of the LDOS [46]. The LDOS can then be expressed via the frequency dependent refractive index n_ω as

$$\rho = \frac{\omega^2}{\pi^2 v_p^2 |v_g|} = \frac{n_\omega^3 \omega^2}{\pi^2 c^3}\left(1 + \frac{\omega}{n_\omega}\frac{dn_\omega}{d\omega}\right). \quad (6)$$

Here v_p and v_g are the phase and group velocities of the electromagnetic wave in the medium, respectively.

In the lossless case but taking into account dispersion of material parameters, the transformation of LDOS for the

respective material parameters transformation is expressed by

$$\rho' = \det{}^{-1}\left(\bar{\bar{A}}\right)\frac{\omega^2}{\pi^2 c^3}\left|1 + \frac{1}{6}\sum_{j=\rho,\varphi,z}\left(\frac{1}{\varepsilon_j}\frac{\mathrm{d}}{\mathrm{d}\omega}\varepsilon_j + \frac{1}{\mu_j}\frac{\mathrm{d}}{\mathrm{d}\omega}\mu_j\right)\right|. \quad (7)$$

We assume that the permittivity of the material can be described by a Drude model $\varepsilon_j(r) = 1 - \left(\omega_{\mathrm{p}j}/\omega\right)^2$ [47], where the damping frequency gamma is zero for lossless case, and the permeability obeys a Lorentz model $\mu_j = 1 - A\omega^2/\left(\omega^2 - \omega_{0j}^2\right)$ [48]. To ensure that the permeability is feasible with metamaterials, here we choose the parameter $A = 0.25$, which corresponds to the filling ratio of the area of the metamaterial structure to that of the unit cell. Using equation (7), we can calculate the transformed LDOS as shown in figure 2(a). (Note that since we assume that the permeability of the materials is given by the Lorentz model, values of μ between $1 - A$ and 1 are not possible in the lossless case. This sets a lower limit to α (i.e., $\alpha > 1/(1 - A)$), so that in figure 2(a) only $\alpha \geqslant 2$ is considered.) In contrast to the nondispersive case, the LDOS increases with α, and for large expansion factors ($\alpha > 4$ in this case), the LDOS is larger than that in free space. As indicated by equation (6), the LDOS increases with the group index of the dispersive material. Large α corresponds to very small (smaller than one) refractive index of the transformed material, which has to be realized with strongly dispersive metamaterial and with high group index.

If we further consider the material loss, equation (7) should be amended as

$$\rho' = \det{}^{-1}\left(\bar{\bar{A}}\right)\frac{\omega^2}{\pi^2 c^3}\left|1 + \frac{1}{6}\sum_{j=\rho,\varphi,z}\left(\frac{1}{\varepsilon_j}\frac{\mathrm{d}}{\mathrm{d}\omega}\varepsilon_j + \frac{1}{\mu_j}\frac{\mathrm{d}}{\mathrm{d}\omega}\mu_j\right)\right|\left|1 - \frac{2}{\pi}\arctan\delta_c\right|, \quad (8)$$

where $\delta_c = \mathrm{Im}(n)/\mathrm{Re}(n)$. Figure 2(b) compares the LDOS in the dispersive anisotropic material with different losses, showing that the inclusion of damping results in the decrease of the LDOS. It should be underlined that an emitter cannot have a direct contact with a lossy media. Mathematically it will result in a diverging energy due to the dissipation or, in other words, diverging imaginary part of electromagnetic Green's function at the emitter's point. In order to prevent this unphysical result, depolarization volumes of lossless materials around emitters are imposed [49].

Engineering the SE rate with optical devices

The considerations above indicate that we can take advantage of the flexibility offered by transformation optics to design devices that can control the SE rate as desired by engineering the distortion of space, i.e., its refractive index profile. We will consider the impact of two transformation optics devices, gradient-index lens and invisibility cloak, on the SE rate.

SE in gradient-refractive-index lens

An all-dielectric gradient-refractive-index lens can magnify subwavelength details of the object and deliver this information to the far-field [29–31]. The gradient-index lens is composed of an isotropic core ($\varepsilon_c = \mu_c = \alpha$ for $r < R_1$) and a matching layer ($R_1 < r < R_2$) with anisotropic gradient index materials. It can be designed by applying the transformation function

$$f(r) = \begin{cases} \alpha r, & \text{when } r < R_1, \\ \dfrac{R_2 - \alpha R_1}{R_2 - R_1}\left(r - R_1\right) + \alpha R_1, & \text{when } R_1 < r < R_2, \end{cases} \quad (9)$$

where the constant α stands for the magnification/shrink factor of the lens. This design gives $\varepsilon_t = \mu_t = f'(r)$, $\varepsilon_r = \mu_r = \varepsilon_0\frac{f^2(r)}{r^2 f'(r)}$.

According to equation (5), the SE rate here is directly related to the compression/expansion of space and enhanced/suppressed by a factor of α^2 in the absence of absorption. We consider the case of a emitter such as a quantum dot or dye molecule with a dipole transition, placed within the core of the lens where $R_2 = 3R_1$. Figure 3(a) shows the Purcell factor for this lens, where we can observe a monotonic increase of the SE rate with the increase of α (note that the horizontal and vertical axes are given in log scales). In particular, when the refractive index of the inner core is smaller than 1 ($n_c = \varepsilon_c = \mu_c = \alpha < 1$), the lens generates a shrunken image and the SE rate is suppressed. Figures 3(b) and (c) show the LDOS in the lenses with different magnification/shrink factors normalized by the LDOS in free space. In the case $\alpha = 2.5$, corresponding to $n_c = 2.5$ in the core, the LDOS decreases at the outer boundary of the lens while gradually increasing to a very large value at the core: the space is compressed in the core whereas expanded at the shell. In contrast, for $\alpha = n_c = 0.05$, the LDOS increases at the outer boundary of the device (where the space is compressed most) with a gradual decrease towards inner boundary, where the LDOS reaches the minimum value close to zero. Figures 3(d)–(f) show the snapshot of the magnetic field distribution in different cases. Compared to a dipole emitter in free space (figure 3(d)), the SE is enhanced when the dipole is embedded in the core of the lens with refractive index $n_c = 2.5$ (figure 3(e)), enabling the subwavelength information to be delivered to the far-field. For a lens with $n_c = 0.05$, the emission in the far-field is dramatically suppressed (figure 3(f)).

The impact of invisibility cloak on SE rate

We now consider an extreme case of equation (9) when $\alpha = 0$. The resulting device is known as the invisibility cloak [24–27]. We study the SE of the dipole placed inside the invisibility cloak [45]. For the nondispersive and lossless

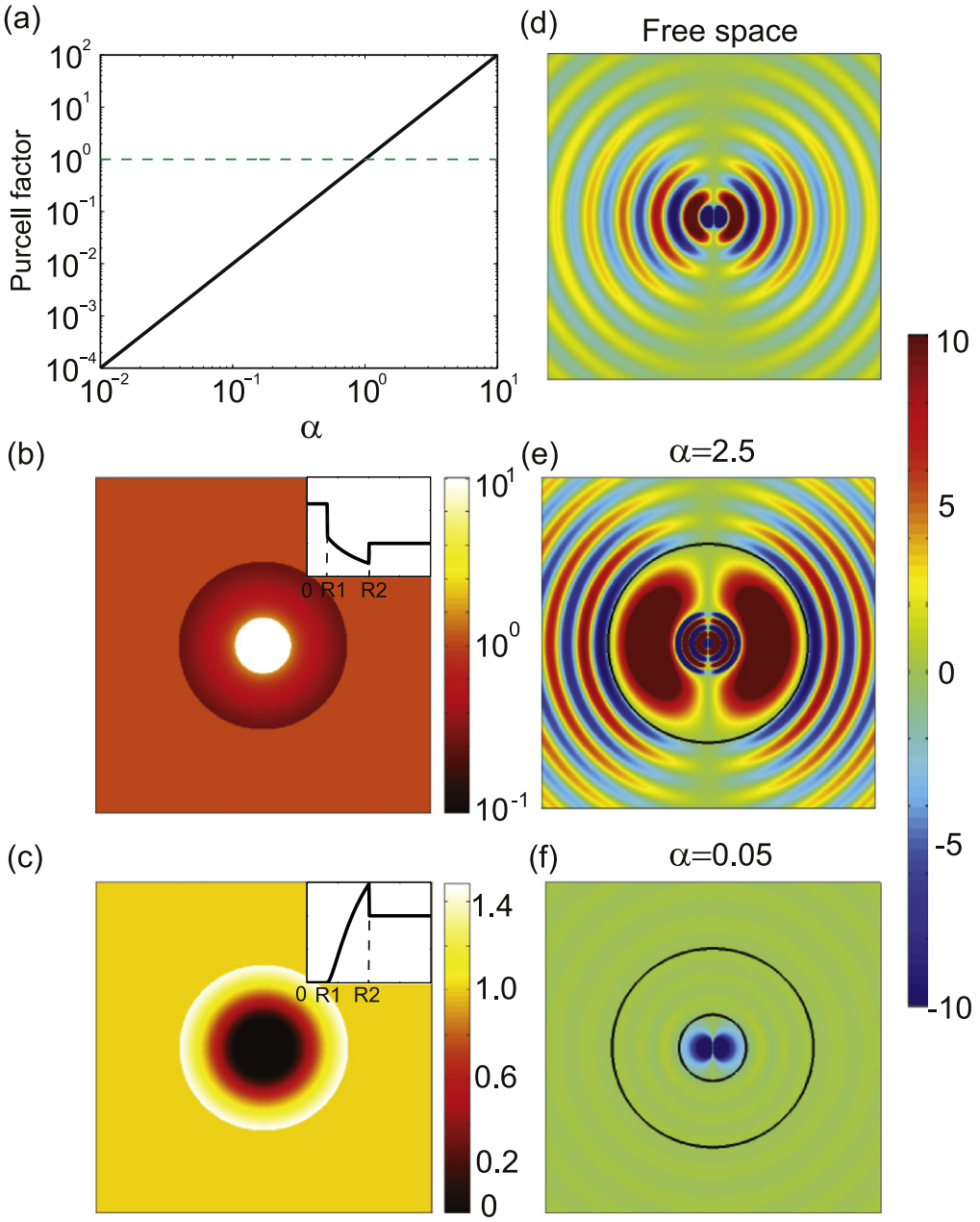

Figure 3. (a) Purcell factor dependence on magnification/shrink factor α for the gradient index lens. (b), (c) The LDOS in the gradient index lenses with different magnification/shrink factors: $\alpha = 2.5$ (b) and $\alpha = 0.05$ (c), normalized to its value in the free space. (d)–(f) The magnetic field distribution for a dipolar emitter in the free space (d) and in the gradient index lenses with different magnification/shrink factors: $\alpha = 2.5$ (e) and $\alpha = 0.05$ (f).

case, the LDOS can be written as

$$\rho' = \det{}^{-1}\left(\bar{\bar{A}}\right)\rho = \frac{\omega^2}{\pi^2 c^3}\left(\frac{R_2}{R_2 - R_1}\right)^2 \frac{r - R_1}{r}. \qquad (10)$$

The LDOS around and inside the cloaked region is shown in figure 4(a), where the LDOS of a cloak shell is shown normalized to its value in free space. In these calculations, the inner radius of the cloak R_1 is chosen to be equal to the working wavelength of the cloak and the outer radius $R_2 = 2R_1$. It should be noted that the radius of the cloak is not directly related to the working frequency of the cloak due to properties of the coordinate transformation and in principle, can be as large as needed. The SE rate of the dipole inside the medium forming the cloak moderately increases at the outer boundary of the cloak (where the space is compressed most) with a gradual decrease towards inner boundary, where the LDOS reaches zero. Inside the cloaked region, the LDOS is zero since in a perfect cloak, the inner cloak boundary is transformed from a line by expanding the space, so that SE is completely suppressed.

In practical realizations, however, the cloak design requires dispersive metamaterials so that every given design works in a relatively narrowband regime. Assuming the same

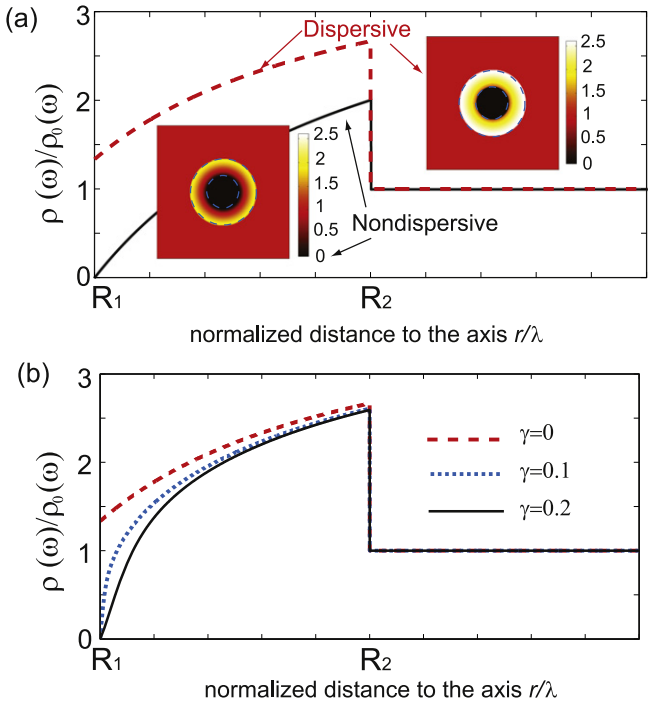

Figure 4. LDOS in and around the cloaked space. (a) The comparison of dispersive and nondispersive cases without dissipation, where the inserts show the LDOS distribution in the cloak shell, and the blue dashed lines indicate the contours of the cloak. (b) LDOS in dispersive media with different damping frequencies.

model for material permittivity and permeability as above, a Drude model and a Lorentz model, respectively, and neglecting losses (equation (8)), the LDOS in the cloak shell is slightly higher compared to the nondispersive case (figure 4(a)). However, it still decreases along the radial direction from the outer to the inner boundary. We note that the LDOS in the dispersive case is no longer zero inside the clock. This is because the extreme value (zero in radial direction, and infinity in angular direction) of the permittivity and permeability reached at the boundary requires strong material dispersion to achieve. However, we find that the losses in the material suppresses the LDOS, especially at the inner boundary of the cloak where the LDOS can reach very small values (figure 4(b)).

The influence of the material loss on the LDOS and Purcell factor is accounted for using full-vectorial numerical simulations (COMSOL Multiphysics), and the SE rate is considered by analyzing the far-field integral of the radiated power. Figure 5(a) shows the dependence of the Purcell factor on the losses in the cloak shell, where we find that increasing the loss leads to an increase of the Purcell factor. This is because the absorption gives rise to the redistribution of states in the system while the number of total photon states is conserved. The extreme case is the lossless ideal cloak in which the SE of a dipole is completely suppressed, as discussed above. For very small losses ($\mathrm{Im}\{\varepsilon_r\} < 0.02$), the SE rate increases rapidly with the material loss, but for $\mathrm{Im}\{\varepsilon_r\} > 0.02$, the SE rate is less sensitive to loss. Figure 5(c) shows the snapshot of the electric field distribution for the emitter located inside the cloak, where the emission is completely inhibited and no radiation can be observed in the far field. This is due to the high electric and magnetic surface voltages achieved due to the required material properties at the inner boundary of a spherical cloak, which prevent electromagnetic waves from going out [50]. When some loss is present in the cloak layer, the emission outside the cloak is clearly observed but still suppressed compared to the free space (figure 5(b)).

In fact, equation (2) indicates that the SE rate depends not only on the distortion of space, but also on the orientation of an emitting dipole in an anisotropic environment. Thus, if we implement a device by compressing the space in one direction while expanding it in the other, we may achieve directional control of SE within this single device. The spherical cloak resulting from compressing a spherical region into an annulus one, involves a compression in the radial direction and expansion in the angular direction, and thus provides a good candidate for this purpose. Figure 6 depicts the dependence of the SE rate enhancement on the orientation of the dipole emitter located at the inner boundary of the cloak. We find that the emission of a dipole oriented parallel to the inner surface of the cloak can be completely suppressed, and the SE rate is gradually increased as the orientation of the dipole rotates towards the normal of the inner surface. This phenomenon can be understood with equation (3): since the inner boundary of the cloak is transformed from a point [25], the angular direction is infinitely expanded ($\alpha = 0$), corresponding to a complete suppression of SE.

Figure 7 shows the magnetic field distributions for emitters located at the inner boundary of the cloak with two different orientations, i.e., parallel and perpendicular to the surface, along which the minimum and maximum emission rates are attained. When the dipole is oriented parallel to the surface, the presence of the loss results in a minor change of the SE rate and leads to the radiation to the far field. Similarly, the emission of the dipole normal to the inner surface can be further enhanced in the presence of damping in the cloak layer. Note that the cloak has the same effect on the directional control of the emission rate of a magnetic-dipole emitters. Control over the orientation of the transition dipole moment allows novel applications where the emission can be switched from enhanced to inhibited by tuning the orientation of an emitter [51].

Conclusion

We have shown that transformation optics offers immense opportunities for designing emission properties in material environment. By appropriately choosing the transformation, control of both the emission rate and directionality can be achieved. The application of the approach is not restricted to the discussed examples of gradient-index lens and cylindrical cloak which are transformed from free space. More complicated cases can be considered starting from an inhomogeneous surroundings before transformation. This opens up a possibility to control the SE inside the transformation optics devices, including invisibility cloaks, using metamaterials. These opportunities can further be extended to active control

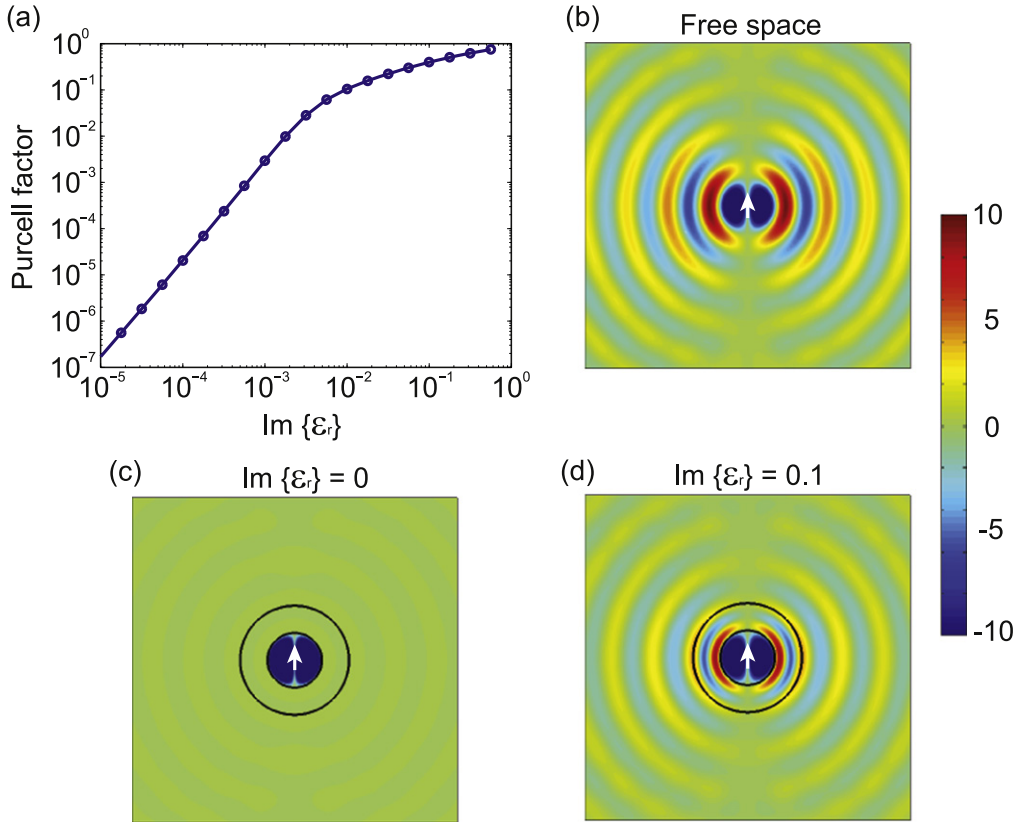

Figure 5. (a) The dependence of the Purcell factor on material loss for the spherical cloak. The emitter is placed inside the cloak. (b)–(d) The magnetic field distribution for a dipole radiating in free space (b) and inside a spherical cloak in the lossless (c) case and in the presence of the material loss $\mathrm{Im}\{\varepsilon_r\} = 0.1$ (d).

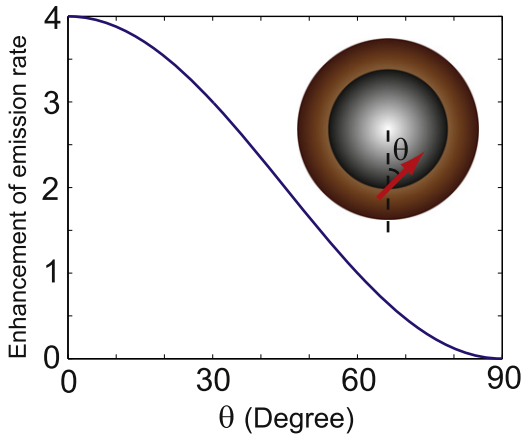

Figure 6. Dependence of the Purcell factor on the angle between the emitting dipole and the normal of the inner surface of the cloak.

of the SE if externally tuneable metamaterials are applied. The presented results may also find applications in various fields including solar energy, illumination, displays, and quantum-information processing.

Acknowledgments

This work was supported, in part, by EPSRC (UK), the Danish Council for Independent Research (Project 1323-00087), Danish Research Council for Technology and Production Sciences (FTP grants #11-104559 and DNRF58), and the ERC iPLASMM Project (No. 321268). J Z and P G were supported by the Royal Society Newton International Fellowships. A Z acknowledges support from the Royal Society and the Wolfson Foundation. G W acknowledges the support from the EC FP7 Project No. 304179 (Marie Curie Actions). The authors acknowledge Asger Mortensen for stimulating discussions. The data access statement: all data supporting this research are provided in full in the results section.

Appendix

A1. Derivation of the LDOS in the transformed space

LDOS describes the number of allowed states at a certain frequency within the volume $[k_\omega, k_{\omega+\Delta\omega}]$ in the k space:

$$\rho = \frac{1}{\pi^3}\frac{\mathrm{d}\Omega_{k(\omega)}}{\mathrm{d}\omega}, \tag{A1}$$

where ω is the angular frequency of the electromagnetic wave and $\Omega_{k(\omega)}$ represents the volume that are contained within the equal-frequency contour k_ω.

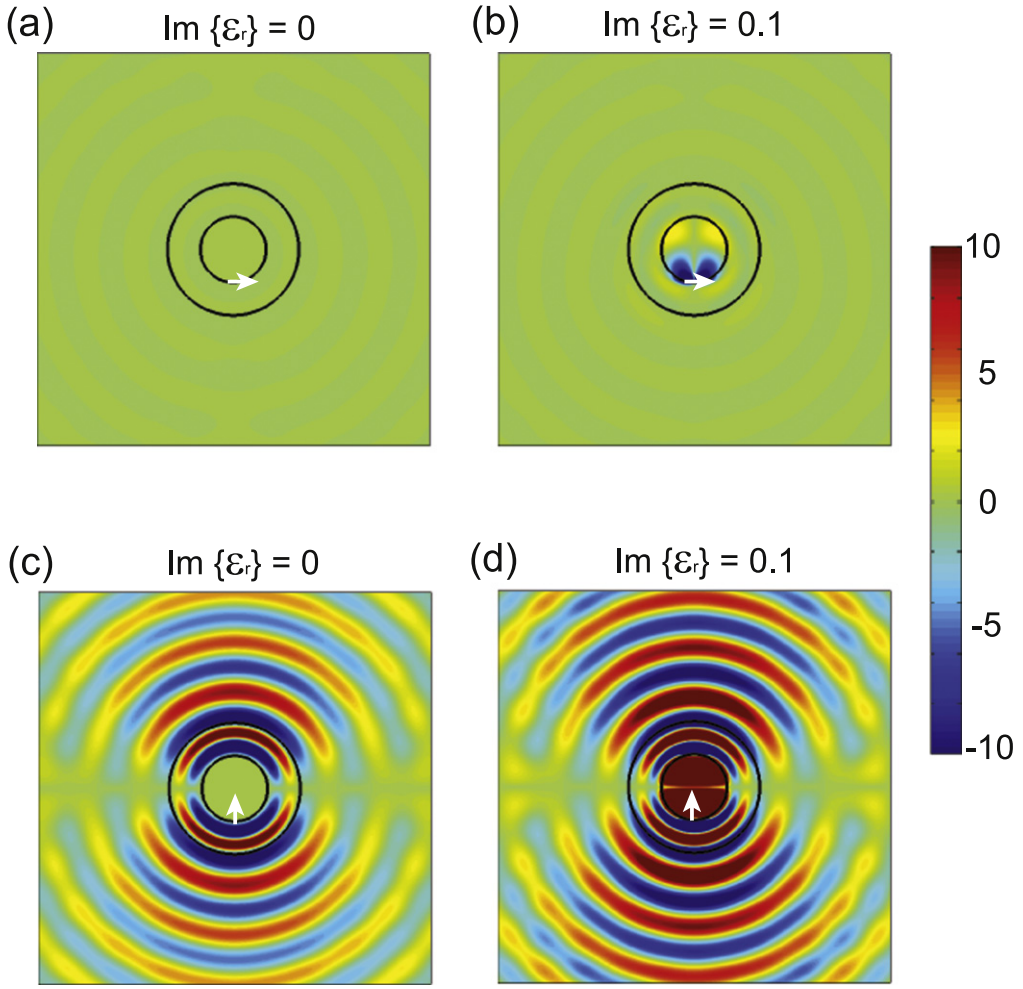

Figure 7. Magnetic field distributions generated by the emitted placed in a cloaked region at the inner boundary of the cloak (a), (b) parallel and (c), (d) perpendicular to the surface for (a), (c) lossless and (b), (d) lossy ($\mathrm{Im}\{\varepsilon_r\} = 0.1$) material.

We shall study how the LDOS is modified under a transformation that maps the space $(x,\ y,\ z)$ to the space $(x',\ y',\ z')$. If $A = \partial(x',\ y',\ z')/\partial(x,\ y,\ z)$ is the Jacobian matrix of the transformation function, then $\mathrm{d}\bar{r}' = \bar{\bar{A}} \cdot \mathrm{d}\bar{r}$. The quantity $\bar{k} \cdot \bar{r}$ must remain unchanged under the transformation. Therefore, the wave vector in the transformed frame can be calculated as $\bar{k}' = (A^T)^{-1}\bar{k}$, so that $\Omega'_{k'(\omega)} = \Omega_{k(\omega)}/\det(\bar{\bar{A}})$. Therefore, in the transformed space, the LDOS is given by

$$\rho' = \det{}^{-1}\left(\bar{\bar{A}}\right)\rho. \tag{A2}$$

The compression of the space leads to the increase of LDOS while the expansion of space corresponds to the decrease of LDOS.

A2. Derivation of the SE rate in the transformed space

To calculate the change of SE rate, we first study how the LDOS is modified under a transformation that maps the space $(x,\ y,\ z)$ to the space $(x',\ y',\ z')$, and $\bar{\bar{A}} = \partial(x',\ y',\ z')/\partial(x,\ y,\ z)$ is the Jacobian matrix of the transformation function.

The electric (magnetic) field can be calculated from the electric (magnetic) current density using the Green's function [1]:

$$E(r) = \mathrm{i}\mu_0\omega \iiint \overleftrightarrow{G}^E(r,\ r_0) \cdot j(r_0)\mathrm{d}^3 r_0, \tag{A3}$$

$$H(\bar{r}) = \iiint \overleftrightarrow{G}^H(r,\ r_0) \cdot m(r_0)\mathrm{d}^3 r_0. \tag{A4}$$

Transformation rules for the fields E and H, and j, m and r_0 are [52]

$$E' = \left(A^T\right)^{-1}E,\ H' = \left(A^T\right)^{-1}H, \tag{A5}$$

$$j' = [\det(A)]^{-1}A \cdot j,\ m' = [\det(A)]^{-1}A \cdot m, \tag{A6}$$

$$\mathrm{d}^3 r'_0 = \det(A)\mathrm{d}^3 r_0. \tag{A7}$$

Substituting equations (A5)–(A7) in equation (A3) and (A4), one finds

$$A^T \cdot E'(r') = \mathrm{i}\mu_0\omega \iiint \overleftrightarrow{G}^E(r,\ r_0) \cdot A^{-1} \cdot j'\left(r'_0\right)\mathrm{d}^3 r'_0, \tag{A8}$$

$$A^T \cdot H'(r') = \iiint \overleftrightarrow{G}^H(r,\ r_0) \cdot A^{-1} \cdot m'(r'_0)\mathrm{d}^3 r'_0. \quad \text{(A9)}$$

Comparing equations (A3), (A4) with (A8), (A9), we obtain

$$\overleftrightarrow{G}^{E'}(r',\ r'_0) = \left(A^T\right)^{-1} \cdot \overleftrightarrow{G}^E(r,\ r_0) \cdot A^{-1}, \quad \text{(A10)}$$

$$\overleftrightarrow{G}^{H'}(r',\ r'_0) = \left(A^T\right)^{-1} \cdot \overleftrightarrow{G}^H(r,\ r_0) \cdot A^{-1}, \quad \text{(A11)}$$

together with the permittivity and permeability tensors

$$\begin{aligned} \varepsilon' &= [\det(A)]^{-1} A \cdot \varepsilon \cdot A^T, \\ \mu' &= [\det(A)]^{-1} A \cdot \mu \cdot A^T. \end{aligned} \quad \text{(A12)}$$

To further verify the validity of equations (A10) and (A11) in a general case, we demonstrate that the transformed Green's function is the solution of Maxwell's equations in anisotropic and inhomogeneous media [53]

$$\begin{aligned} \nabla' \times \bar{E}' &= \mathrm{i}\omega\mu_0 \bar{\bar{\mu}}' \cdot \bar{H}' \\ \nabla' \times \bar{H}' &= -\mathrm{i}\omega\varepsilon_0 \bar{\bar{\varepsilon}}' \cdot \bar{E}' + \bar{J}'. \end{aligned} \quad \text{(A13)}$$

Eliminating the magnetic field $\bar{H}'$, we obtain the following equation for $\bar{E}'$:

$$\nabla' \times \bar{\bar{\mu}}'^{-1} \cdot \nabla' \times \bar{E}' - k_0^2 \bar{\bar{\varepsilon}}' \cdot \bar{E}' = \mathrm{i}\omega\mu_0 \bar{J}'. \quad \text{(A14)}$$

Hence, the differential equation for dyadic Green's function $\bar{\bar{G}}'$ can be written as

$$\nabla' \times \bar{\bar{\mu}}'^{-1} \cdot \nabla' \times \bar{\bar{G}}' - k_0^2 \bar{\bar{\varepsilon}}' \cdot \bar{\bar{G}}' = \bar{\bar{I}}\delta', \quad \text{(A15)}$$

where $\bar{\bar{I}}$ denotes the unit matrix. To simplify the discussion, we assume the original space is vacuum ($\varepsilon = 1$ and $\mu = 1$). From equations (A10) to (A12), we find

$$\begin{aligned} \bar{\bar{\varepsilon}}' &= \bar{\bar{\mu}}' = \det{}^{-1}\left(\bar{\bar{A}}\right)\bar{\bar{A}} \cdot \bar{\bar{A}}^T \\ \bar{\bar{G}}' &= \left(\bar{\bar{A}}^T\right)^{-1} \cdot \bar{\bar{G}} \cdot \bar{\bar{A}}^{-1}. \end{aligned} \quad \text{(A16)}$$

Hence, we only need to demonstrate that $\bar{\bar{G}}$ is the Green's function in vacuum. Using equation (A16), we obtain

$$\begin{aligned} \nabla' \times \bar{\bar{\mu}}'^{-1} \cdot \nabla' \times \bar{\bar{G}}' &= \nabla' \times \det\left(\bar{\bar{A}}\right)\left(\bar{\bar{A}}^T\right)^{-1} \\ &\quad \cdot \bar{\bar{A}}^{-1} \cdot \nabla' \times \left[\left(\bar{\bar{A}}^T\right)^{-1} \cdot \bar{\bar{G}} \cdot \bar{\bar{A}}^{-1}\right] \\ &= \nabla' \times \left(\bar{\bar{A}}^T\right)^{-1} \cdot \nabla \times \bar{\bar{G}} \cdot \bar{\bar{A}}^{-1} \\ &= \det{}^{-1}\left(\bar{\bar{A}}\right)\bar{\bar{A}} \cdot \nabla \times \nabla \times \bar{\bar{G}} \cdot \bar{\bar{A}}^{-1}, \end{aligned} \quad \text{(A17)}$$

$$\begin{aligned} \bar{\bar{\varepsilon}}' \cdot \bar{\bar{G}}' &= \det{}^{-1}\left(\bar{\bar{A}}\right)\bar{\bar{A}} \cdot \bar{\bar{A}}^T \cdot \left[\left(\bar{\bar{A}}^T\right)^{-1} \cdot \bar{\bar{G}} \cdot \bar{\bar{A}}^{-1}\right] \\ &= \det{}^{-1}\left(\bar{\bar{A}}\right)\bar{\bar{A}} \cdot \bar{\bar{A}}^T \cdot \left(\bar{\bar{A}}^T\right)^{-1} \cdot \bar{\bar{G}} \cdot \bar{\bar{A}}^{-1} \\ &= \det{}^{-1}\left(\bar{\bar{A}}\right)\bar{\bar{A}} \cdot \bar{\bar{G}} \cdot \bar{\bar{A}}^{-1}. \end{aligned} \quad \text{(A18)}$$

Substituting equations (A17) and (A18) into equation (A15) yields:

$$\begin{aligned} &\det{}^{-1}\left(\bar{\bar{A}}\right)\bar{\bar{A}} \cdot \nabla \times \nabla \times \bar{\bar{G}} \cdot \bar{\bar{A}}^{-1} \\ &\qquad -k_0^2 \det{}^{-1}\left(\bar{\bar{A}}\right)\bar{\bar{A}} \cdot \bar{\bar{G}} \cdot \bar{\bar{A}}^{-1} = \bar{\bar{I}}\delta' \\ &\Leftrightarrow \det{}^{-1}\left(\bar{\bar{A}}\right)\bar{\bar{A}} \cdot \left(\nabla \times \nabla \times \bar{\bar{G}} - k_0^2 \bar{\bar{G}}\right) \cdot \bar{\bar{A}}^{-1} = \bar{\bar{I}}\delta' \\ &\Leftrightarrow \nabla \times \nabla \times \bar{\bar{G}} - k_0^2 \bar{\bar{G}} = \left(\bar{\bar{A}}^{-1} \cdot \bar{\bar{I}} \cdot \bar{\bar{A}}\right)\left[\det\left(\bar{\bar{A}}\right)\delta'\right] \\ &\qquad = \bar{\bar{I}}\delta, \end{aligned} \quad \text{(A19)}$$

where $\delta = \det(\bar{\bar{A}})\delta'$. In this way, we have recovered the differential equation of the Green's function in free space. This indicates that the Green's function given by equation (A16) is a solution of the wave equation given by equation (A15), in agreement with our previous derivation. It can analogously be shown explicitly that the transformed magnetic Green function indeed has the form of equation (A11).

In the transformed space (x', y', z'), the operational definition of the SE rate of an emitting dipole p with a dipole moment p' in the transformed space can be calculated as

$$\begin{aligned} \Gamma' &= \left\langle p'^T \cdot \mathrm{Im}\left\{\overleftrightarrow{G}'(\bar{r},\ \bar{r}_0)\right\} \cdot p' \right\rangle = \left\langle \left(A^{-1}p'\right)^T \right. \\ &\quad \left. \cdot \mathrm{Im}\left\{\overleftrightarrow{G}(\bar{r},\ \bar{r}_0)\right\} \cdot \left(A^{-1}p'\right) \right\rangle. \end{aligned} \quad \text{(A20)}$$

This equation indicates that the emitting dipole located in the transformed medium has exactly the same radiation properties as a dipole in the original space whose dipole moment is given by $p = A^{-1} \cdot p'$. In particular, if the original space is free space, by substituting the free space Green's function in equation (A13), the transformed SE rate can be obtained as

$$\Gamma' = \frac{\omega^3 |A^{-1} \cdot p'|^2}{3\pi\varepsilon_0 \hbar c_0^3} = \frac{|A^{-1} \cdot p'|^2}{|p'|^2}\Gamma, \quad \text{(A21)}$$

where Γ is the SE rate of the emitter in free space.

References

[1] Novotny L and Hecht B 2006 *Principles of Nano-Optics* (Cambridge: Cambridge University Press)

[2] Russell K J, Liu T-L, Cui S and Hu E L 2012 Large spontaneous emission enhancement in plasmonic nanocavities *Nat. Photonics* **6** 459

[3] Denisyuk A I, Adamo G, MacDonald K F, Edgar J, Arnold M D, Myroshnychenko V, Ford M J, García de Abajo F J and Zheludev N I 2010 Transmitting hertzian optical nanoantenna with free-electron feed *Nano Lett.* **10** 3250

[4] Snoeks E, Lagendijk A and Polman A 1995 Measuring and modifying the spontaneous emission rate of erbium near an interface *Phys. Rev. Lett.* **74** 2459

[5] Joulain K, Carminati R, Mulet J-P and Greffet J-J 2003 Definition and measurement of the local density of electromagnetic states close to an interface *Phys. Rev.* B **68** 245405

[6] Shields A J 2007 Semiconductor quantum light sources *Nat. Photonics* **1** 215

[7] Li Z Y, Lin L L and Zhang Z Q 2000 Spontaneous emission from photonic crystals: full vectorial calculations *Phys. Rev. Lett.* **84** 4341

[8] Englund D, Fattal D, Waks E, Solomon G, Zhang B, Nakaoka T, Arakawa Y, Yamamoto Y and Vučković J 2005 Controlling the spontaneous emission rate of single quantum dots in a two-dimensional photonic crystal *Phys. Rev. Lett.* **95** 013904

[9] Lodahl P, Floris van Driel A, Nikolaev I S, Irman A, Overgaag K, Vanmaekelbergh D and Vos W L 2004 Controlling the dynamics of spontaneous emission from quantum dots by photonic crystals *Nature* **430** 654–7

[10] Colas des Francs G, Grandidier J, Massenot S, Bouhelier A, Weeber J-C and Dereux A 2009 Integrated plasmonic waveguides: a mode solver based on density of states formulation *Phys. Rev.* B **80** 115419

[11] Farahani J N, Pohl D W, Eisler H-J and Hecht B 2005 Single quantum dot coupled to a scanning optical antenna: a tunable superemitter *Phys. Rev. Lett.* **95** 017402

[12] Taminiau T H, Stefani F D, Segerink F B and van Hulst N F 2008 *Nat. Photonics* **2** 234

[13] Gérard J M, Sermage B, Gayral B, Legrand B, Costard E and Thierry-Mieg V 1998 Enhanced spontaneous emission by quantum boxes in a monolithic optical microcavity *Phys. Rev. Lett.* **81** 1110

[14] Noginov M A, Li H, Barnakov Y A, Dryden D, Nataraj G, Zhu G, Bonner C E, Mayy M, Jacob Z and Narimanov E E 2010 Controlling spontaneous emission with metamaterials *Opt. Lett.* **35** 1863

[15] Ginzburg P, Krasavin A V, Richards D and Zayats A V 2014 Impact of nonradiative line broadening on emission in photonic and plasmonic cavities *Phys. Rev.* A **90** 043836

[16] Purcell E M 1946 *Proc. American Physical Society Phys. Rev.* **69** 674

[17] Yan W, Wubs M and Mortensen N A 2012 Hyperbolic metamaterials: nonlocal response regularizes broadband supersingularity *Phys. Rev.* B **86** 205429

[18] Poddubny A N, Belov P A, Ginzburg P, Zayats A V and Kivshar Y S 2012 Microscopic model of Purcell enhancement in hyperbolic metamaterials *Phys. Rev.* B **86** 035148

[19] Slobozhanyuk A P *et al* 2015 Purcell effect in hyperbolic metamaterial resonators *Phys. Rev.* B **92** 195127

[20] Luo J, Lu W, Hang Z, Chen H, Hou B, Lai Y and Chan C T 2014 Arbitrary control of electromagnetic flux in inhomogeneous anisotropic media with near-zero index *Phys. Rev. Lett.* **112** 073903

[21] Shalin A S, Ginzburg P, Orlov A A, Iorsh I, Belov P A, Kivshar Y S and Zayats A V 2015 Scattering suppression from arbitrary objects in spatially dispersive layered metamaterials *Phys. Rev.* B **91** 125426

[22] Gu J-D 2003 Microbiological deterioration and degradation of synthetic polymeric materials: recent research advances *Int. Biodeterioration Biodegradation* **52** 69

[23] Poddubny A N, Ginzburg P, Belov P A, Zayats A V and Kivshar Y S 2012 Tailoring and enhancing spontaneous two-photon emission using resonant plasmonic nanostructures *Phys. Rev.* A **86** 033826

[24] Leonhardt U 2006 Optical conformal mapping *Science* **312** 1777

[25] Pendry J B, Schurig D and Smith D R 2006 Controlling electromagnetic fields *Science* **312** 1780

[26] Cummer S A, Popa B-I, Schurig D, Smith D R and Pendry J B 2006 Full-wave simulations of electromagnetic cloaking structures *Phys. Rev.* E **74** 036621

[27] Luo Y, Chen H, Zhang J, Ran L and Kong J A 2008 Design and analytical full-wave validation of the invisibility cloaks, concentrators, and field rotators created with a general class of transformations *Phys. Rev.* B **77** 125127

[28] Zhang J, Luo Y and Mortensen N A 2010 Minimizing the scattering of a nonmagnetic cloak *Appl. Phys. Lett.* **96** 113511

[29] Jiang W X, Qiu C-W, Han T C, Cheng Q, Ma H F, Zhang S and Cui T J 2013 Broadband all-dielectric magnifying lens for far-field high-resolution imaging *Adv. Mater.* **25** 6963–8

[30] Zhang B and Barbastathis L G 2010 Dielectric metamaterial magnifier creating a virtual color image with far-field subwavelength information *Opt. Express* **18** 11216

[31] Zhang J 2015 Evolutionary optimization of compact dielectric lens for farfield sub-wavelength imaging *Sci. Rep.* **5** 10083

[32] Zhang J, Luo Y, Chen H and Wu B-I 2008 Manipulating the directivity of antennas with metamaterial *Opt. Express* **16** 10962

[33] Luo Y, Zhang J, Chen H, Huangfu J and Ran L 2009 High-directivity antenna with small antenna aperture *Appl. Phys. Lett.* **95** 193506

[34] Zhang J, Xiao S, Wubs M and Mortensen N A 2011 Surface plasmon wave adapter designed with transformation optics *ACS Nano* **5** 4359

[35] Luo Y, Pendry J B and Aubry A 2010 Surface plasmons and singularities *Nano Lett.* **10** 4186

[36] Luo Y, Lei D Y, Maier S A and Pendry J B 2012 Broadband light harvesting nanostructures robust to edge bluntness *Phys. Rev. Lett.* **108** 023901

[37] Luo Y, Aubry A and Pendry J B 2011 Electromagnetic contribution to surface-enhanced Raman scattering from rough metal surfaces: a transformation optics approach *Phys. Rev.* B **83** 155422

[38] Pendry J B, Yu Luo and Zhao R 2015 Transforming the optical landscape *Science* **348** 521–4

[39] Yu Luo R, Zhao and Pendry J B 2014 van der Waals interactions at the nanoscale: the effects of non-locality *Proc. Natl Acad. Sci. USA* **111** 18422–7

[40] Kraft M, Luo Y, Maier S A and Pendry J B 2015 Designing plasmonic gratings with transformation optics *Phys. Rev.* X **5** 031029

[41] Smith D R, Pendry J B and Wiltshire M C K 2004 Metamaterials and negative refractive index *Science* **305** 788

[42] Boroditsky M, Vrijen R, Krauss T F, Coccioli R, Bhat R and Yablonovitch E 1999 Spontaneous emission extraction and Purcell enhancement from thin-film 2D photonic crystals *J. Lightwave Technol.* **17** 2096–112

[43] Barnett S M, Huttner B and Loudon R 1992 Spontaneous emission in absorbing dielectric media *Phys. Rev. Lett.* **68** 3698

[44] Milonni P W and Maclay G J 2003 Quantized-field description of light negative-index media *Opt. Commun.* **228** 161–5

[45] Aubry A and Pendry J 2013 *Active Plasmonics and Tuneable Metamaterials* (New York: Wiley)

[46] Milonni P W 1995 Field quantization and radiative processes in dispersive dielectric media *J. Mod. Opt.* **42** 1991–2004

[47] Drude P 1900 Zur elektronentheorie der metalle *Ann. Phys., Lpz.* **306** 566–613

[48] Lorenz E 1963 *J. Atmos. Sci.* **20** 130

[49] Kort-Kamp W J M, Rosa F S S, Pinheiro F A and Farina C 2013 Spontaneous emission in the presence of a spherical plasmonic metamaterial *Phys. Rev.* A **87** 023837

[50] Zhang B, Chen H, Wu B I and Kong J A 2008 Extraordinary surface voltage effect in the invisibility cloak with an active device inside *Phys. Rev. Lett.* **100** 063904

[51] Vos W L, Koenderink A F and Nikolaev I S 2009 Orientation-dependent spontaneous emission rates of a two-level

quantum emitter in any nanophotonic environment *Phys. Rev.* A **80** 053802

[52] Kundtz N B, Smith D R and Pendry J B 2011 Electromagnetic design with transformation optics *Proc. IEEE* **99** 1622–33

[53] Luo Y, Zhang J, Ran L, Chen H and Kong J A 2008 New concept conformal antennas utilizing metamaterial and transformation optics *IEEE Antennas Wirel. Propag. Lett.* **7** 509–12